ArcelorMittal Liège
Research and Development

18 février 2009.

GIORGIA CAROLI
Steel Solutions Design Construction
Phone : +32 (0) 42.36.88.11
Mail : ArcelorResearchLiege@arcelormittal.com

Report

Project :ROBUST
FA : CA 37436
Applicant :

Ref: GCR9001R

Recipients :
Liste des destinataires
Bibliothèque.

double skin facade

ROBUST

Keywords: Termes techniques, n° étude, nom produit, ...
Market: Construction Batiment (CB)
Product-Process: non défini (ND)
Company:

Content :

ROBUST Double skin façades

Abstract: We propose an investigation of the thermo-convective flow in a double-skin wall based on the stacking of a thin steel wall, an air slab and a solid wall made of an insulation material and concrete. The Fluent software is used to analyse the natural convection phenomenon in the air layer and the heat transfer in the fluid and the solid zones, included in the thin steel wall and the fixings that ensure the assembly stiffness. We compare the stacking system with a reference wall in terms of heat transfer capacity, for various concrete layer thicknesses.

GIORGIA CAROLI

Table of content

1. Double skin facades- introduction

In the frame of the ROBUST project, ArcelorMittal investigates the use of steel technologies in the renovation, the adaptation and the upgrading of existing buildings. By the use of a cladding technique, ArcelorMittal plans to solve some specific issues such as the thermal performance enhancements or the water penetration reduction. In that purpose, Cenaero has performed a numerical study of the thermo-convective flow inside of a double-skin wall for ArcelorMittal.

After a definition of the double skin concept, a description of the stacking and its environment, an optimized meshing of the calculation domain is presented. The thermo convective flow in the double-skin wall is investigated and it is compared with a reference wall in terms of heat transfer capacity, for various concrete layer thicknesses.

1.1 Definition

> "An active façade is a façade covering one or several storeys constructed with multiple glazed skins. The skins can be air tighten or not. In this kind of façade, the air cavity situated between the skins is naturally or mechanically ventilated. The air cavity ventilation strategy may vary with the time. Devices and systems are generally integrated in order to improve the indoor climate with active or passive techniques. Most of the time such systems are managed in semi automatic way via control systems." BBRI (2002)

> "Double Skin Façade system is essentially a pair of glass "skins" separated by an air corridor. The main layer of glass is usually insulating. The air space between the layers of glass acts as insulation against temperature extremes, winds, and sound. Sun-shading devices are often located between the two skins. All elements can be arranged differently into numbers of permutations and combinations of both solid and diaphanous membranes". Harrison and Boake, (2003)

> "Double Skin Façade is a façade that consists of two distinct planar elements that allows interior or exterior air to move through the system. This is sometimes referred to as a twin skin." Arons, (2001)

> "A second skin façade is an additional building envelope installed over the existing façade. This additional façade is mainly transparent. The new space between the second skin and the original façade is a buffer zone that serves to insulate the building. This buffer space may also be heated by solar radiation, depending on the orientation of the façade. For south oriented systems, this solar heated air is used for heating purposes in the winter time. It must be vented in order to prevent overheating in other periods." Claessens and DeHerde

1.2 Classification

Different ways to classify Double Skin Façade Systems are mentioned in the literature. The systems can be categorized by the type of construction, the origin, destination and type of the air flow in the cavity, etc. The Environmental Engineering firm of Battle McCarthy in Great Britain created a categorization of five primary types (plus sub-classifications) based on commonalities of façade configuration and the manner of operation. These are:

- Category A: Sealed Inner Skin: subdivided into mechanically ventilated cavity with controlled flue intake versus a ventilated and serviced thermal flue.
- Category B: Openable Inner and Outer Skins: subdivided into single story cavity height versus full building cavity height.
- Category C: Openable Inner Skin with mechanically ventilated cavity with controlled flue intake
- Category D: Sealed Cavity, either zoned floor by floor or with a full height cavity.
- Category E: Acoustic Barrier with either a massive exterior envelope or a lightweight exterior envelope.

In this report we will focus on the use of double skin facades for renovation pourpouses therefore on the categories C, D, E

1.3 Double skin facades and ventilation

Kragh, (2000) categorizes the Double Skin Facades according to the function (ventilation type) of the cavity in three types:

- Naturally Ventilated Wall: “An extra skin is added to the outside of the building envelope. In periods with no solar radiation, the extra skin provides additional thermal insulation. In periods with solar irradiation, the skin is naturally ventilated from/to the outside by buoyancy (stack) effects - i.e. the air in the cavity rises when heated by the sun (the solar radiation must be absorbed by blinds in the cavity). Solar heat gains are reduced as the warm air is expelled to the outside. The temperature difference between the outside air and the heated air in the cavity must be significant for the system to work. Thus, this type of façade cannot be recommended for hot climates”.

- Active Wall: “An extra skin is applied to the inside of the building envelope; inside return air is passing through the cavity of the façade and returning to the ventilation system. In periods with solar radiation the energy, which is absorbed by the blinds, is removed by ventilation. In periods with heating loads, solar energy can be recovered by means of heat exchangers. Both during cold periods with no or little solar irradiation and during periods with solar gains or cooling loads, the surface temperature of the inner glass is kept close to room temperature, leading to increased occupant comfort in the perimeter zone, near the façade. This type of façade is recommended for cold climates, because of the increased comfort during the cold season and the possible recovery of solar energy”.

- Interactive Wall: “The principle of the interactive is much like that of the naturally ventilated wall with the significant difference that the ventilation is forced. This means that the system works in situations with high ambient temperatures, as it does not depend on the stack effect alone. The system is thus ideal for hot climates with high cooling loads. During cold periods with no solar irradiation (e.g. during night-time) the ventilation can be minimized for increased thermal insulation. Apart from the advantages in terms of solar and thermal performance the system allows the use of operable windows for natural ventilation, even in highrise buildings”.

2. Case description and assumptions

A complete description of the double-skin wall and the so-called reference wall can be found in the technical notes provided by ArcelorMittal (references Igr7019N and GCR7025N). A sketch of both walls is proposed in figure 1.

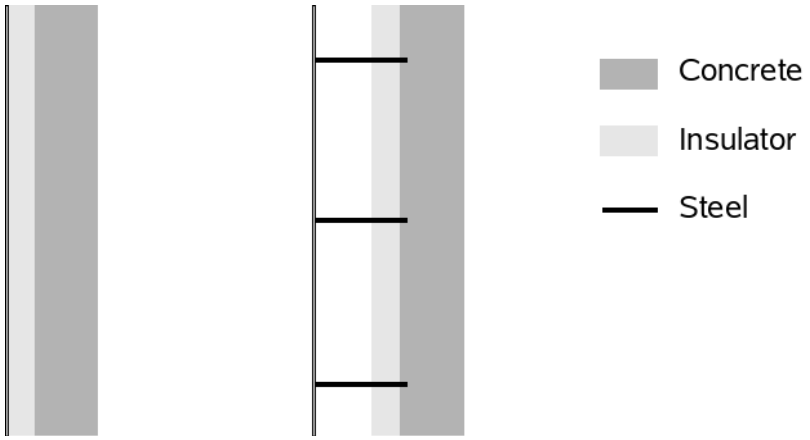

Figure 1: Sketch of the reference wall (left) and the double-skin wall (right)

The walls are based on a three-layer solid slab of steel, insulation material and concrete.
In the double-skin wall configuration, the steel plate and the insulator are separated by an air column. Due to the solar exposure of the steel wall, its temperature increases and a flow is induced by natural convection, affecting the global heat transfer of the stacking. The goal of this study is to evaluate the heat transfer coefficient of the double-skin wall and compare it with the one of the reference wall.
The steel wall is attached by a series of thin steel fixings which ensure the stiffness of the assembly but also a thermal bridge between the external environment and the solid slab. This role will be investigated.
A tri-dimensional detailed view of the double-skin wall is given in section 3.

In this study, we use the following convention to define the heat transfer coefficient. The flux Φ, applied to the steel wall and entering the building, is related to the temperature gradient between the inner concrete wall and the outer steel wall ΔT by:

$$\Phi = S\ U\ \Delta T\ (W)$$

where S is the exchange surface and U [$Wm^{-2}K^{-1}$] is the heat transfer coefficient. Note that we do not take into account the heat transfer with the environment. The properties of the stacking materials are proposed in the following table.

Material	Property	Value
Air	Density (kgm^{-3})	Variable (1.165 at 301.15 K)
	Specific heat ($Jkg^{-1}K^{-1}$)	1006
	Thermal conductivity ($Wm^{-1}K^{-1}$)	0.024
	Thermal expansion coefficient (K^{-1})	3.33 10^{-3} at 301.15 K
Concrete	Density (kgm^{-3})	2300
	Specific heat ($Jkg^{-1}K^{-1}$)	871
	Thermal conductivity ($Wm^{-1}K^{-1}$)	1.75
Insulator	Density (kgm^{-3})	25
	Specific heat ($Jkg^{-1}K^{-1}$)	936
	Thermal conductivity ($Wm^{-1}K^{-1}$)	0.04
Steel	Density (kgm^{-3})	7800
	Specific heat ($Jkg^{-1}K^{-1}$)	447
	Thermal conductivity ($Wm^{-1}K^{-1}$)	50

Table 1: properties of the stacking materials

By neglecting the steel layer due to its high thermal conductivity and its small thickness, the heat transfer coefficient of the reference wall takes the following values, for a fixed insulator thickness (50 mm) and a variable concrete thickness e (mm). Note that in the double-skin wall configuration, the additional air slab introduces a new thermal resistance. The last column of the table estimates the heat transfer coefficient including the effect of the 100 mm-thick layer of incompressible air, in a pure conductive approach.

$e\ (mm)$	$U\ (Wm^{-2}K^{-1})$ (without air)	$U\ (Wm^{-2}K^{-1})$ (with air)
90	0.768	0.183
120	0.758	0.182
150	0.749	0.182
200	0.732	0.181
250	0.717	0.180

Table 2: U value

The U values are estimated by a law of conductance in parallel in a 1D conductive approach :

$$U = \frac{1}{a + (e/k)}$$

with e the thickness in meters, k the concrete thermal conductivity, $a = (1/U_0) - (e_0/k)$ with U_0 the heat transfer coefficient for a thickness $e_0 = 90\ 10^{-3}\ m.$

In this study, the applied flux is due to the solar exposure of the steel skin. This is estimated to 900 Wm^{-2}. It is partially absorbed, depending on the wall absorption coefficient, and partially rejected in the ambient by a radiative and a convective action.
As a result, the wall temperature increases, inducing a natural convection phenomenon in the air layer. This flow brings a fraction of the heat flux out of the domain and therefore reduces the heat load on the insulation and the concrete slabs.

We assume that the heat transfer coefficient (h_{out}) for the combined effect of the radiation and the convection to ambient is 25 $Wm^{-2}\ K^{-1}$. In the same way, the convective heat transfer (h_{in}) from the concrete wall to the indoor is estimated to 7.7 $Wm^{-2}K^{-1}$. The outer temperature (T_{out}) is fixed to 301.15 K (summer conditions) and the inner one (T_{in}) is fixed to 295.15 K.
The steel absorption coefficient α is assumed to be 0.5. This constant value will be used in the first stage of the study (see section 5). In the second stage, we will assume that the use of a radiative coating ensures a linear distribution of this coefficient in the vertical direction. Two opposite configurations will be envisaged in which the coefficient varies from 0.1 to 0.9. The global heat flux imposed to the external steel skin is then estimated as follows:

$$\phi_{in} = \phi_{sol}\ \alpha(y) - h_{in}\ (T_w - T_{out}) \quad (3)$$

where Φ_{in} is the flux in Wm^{-2}, y is the vertical direction, Φ_{sol} is the solar flux in Wm^{-2} and T_w is the steel skin temperature.
All the boundary conditions are summarized in section 4.

3. Phase 1 : CAO and mesh generation

The geometry and the mesh generations were achieved with the GAMBIT software.
The geometry presents a large scale contrast between the skin size and the fixing one. Indeed, the steel skin is 2000 mm high and 900 mm wide and the fixings are 100 mm high and 50 mm wide. Moreover, the steel elements (including the steel skin) are only few millimetres thick.
As a consequence, it was decided that the steel elements would not be meshed in their thickness direction. They are considered as two-dimensional thin walls and the shell conduction model is activated in the Fluent solver in order to take into account the heat conduction inside of them. As the fixings may play a thermal bridge role, we must ensure a good in-plane meshing of the several steel parts. This strongly conditions the mesh choice as this operation drastically increases the meshed element number.

Figure 2 shows a global view of the geometry, including the three steel fixings, for a concrete thickness e of 200 mm. The central fixing extends from z = 0 mm to z = −200 mm, y = −50 mm to y = 50 mm and x = −25 mm to x = 25 mm in the local coordinate system (G_x,G_y, G_z). The two others are shifted of ±750 mm in the vertical direction.

The domain is cut in four layers in the z direction. These layers correspond to the air slab (z = [0,−100] mm), which is bounded by the steel skin at z = 0 mm, the insulation slab (z = [−100,−150] mm), a first fixed-size concrete slab including the steel fixing (z = [−150,−200] mm) and a pure concrete slab of a variable thickness (z = [−200,−200 − (e − 50)] mm), with e the total concrete thickness, as defined in the previous section.

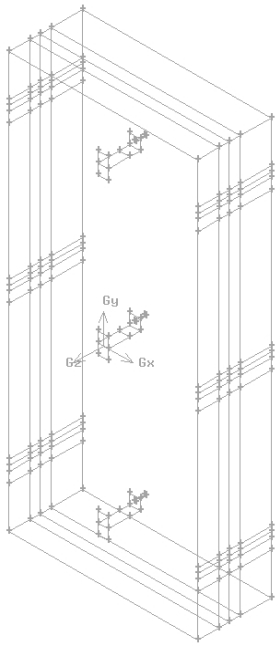

Figure 2: Wall geometry

Figure 3 gives two views of one of the three steel fixing geometry. In the air zone, the steel is 4 mm thick. In the insulation material, the steel is 2 mm thick. In these last cases the plates are 50 mm wide. The last part of the fixing is included in the fixed-size concrete volume. This is a 8 mm-diameter circular part. Nevertheless, as the fixings are not meshed in their thickness direction, this last part has been converted in a square-section object with an equivalent section, so that it has a width and a thickness of 7.09 mm.

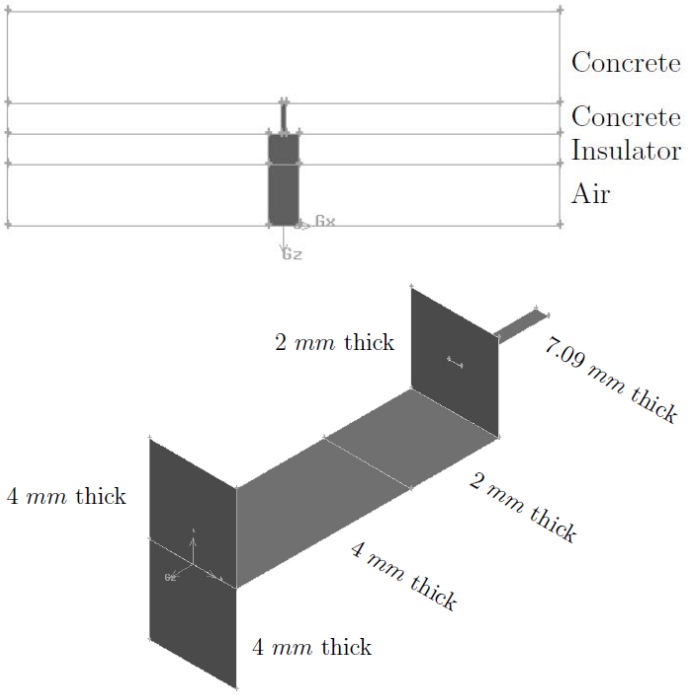

Figure 3: Geometry of the fixing elements

In order to keep a good ratio between an accurate steel fixing discretization and a reasonable meshed element number, we used a hexahedral scheme. It was possible as the geometry is based on square section elements, including the last part of the steel fixing as we reduced the circular section to an equivalent square section. We first meshed the steel skin (z = 0 plane).
We took care to generate a small size mesh on and around the steel fixings. The characterized cell size of the steel fixings is 5 mm. Far from these fixings; the cell size reaches 20 mm. Then, we extruded the mesh in the z direction. We ensured 10 (30) layers in the insulator material (the two concrete zones). The extrusion was performed with a variable interval in the air slab thickness, in order to get a local mesh refinement close to walls (the steel skin and the air/insulator interface). A special refinement was achieved around the steel skin as the temperature and the velocity gradients are of high importance in that zone. We ensured 45 layers in air with a layer growth rate of 1.2 from the steel skin and 1.05 from the insulator interface.
Figures 4,5 and 6 illustrate the mesh in the planes normal to the z, y and x directions, respectively.

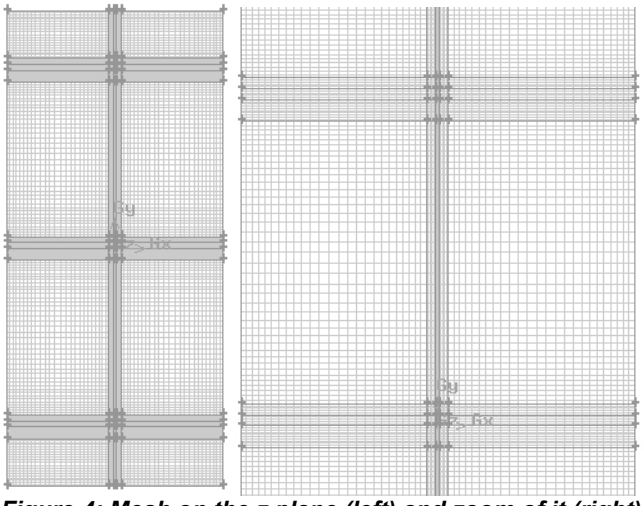

Figure 4: Mesh on the z plane (left) and zoom of it (right)

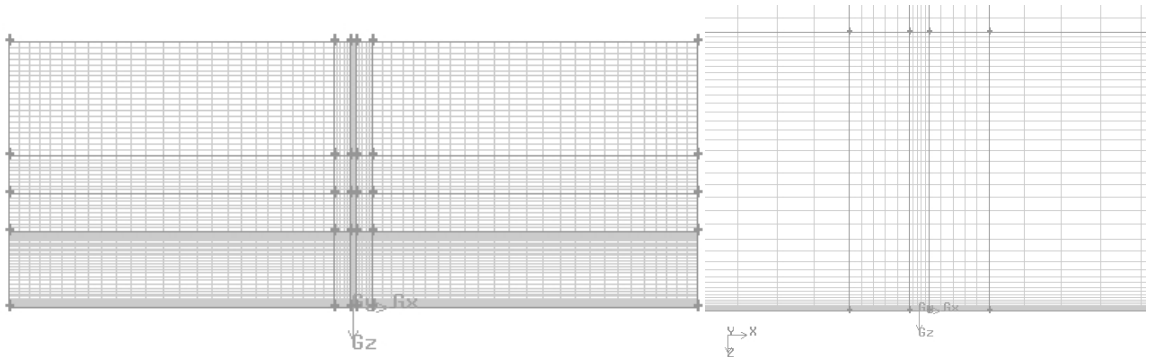

Figure 5: Mesh in the y-plane (left) and zoom on it (right)

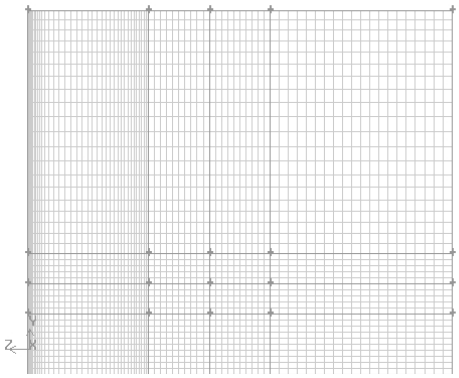

Figure 6: Mesh in the x- plane

Figure 7 shows the resulting mesh on a steel fixing. As mentioned above, the characteristic cell size is 5 mm. Nevertheless, we ensured five mesh points in the thinnest fixing part (in the concrete slab) so that the cell size is locally reduced to 7.08/5 = 1.42 mm. The resulting global mesh contains 1.000.000 elements.

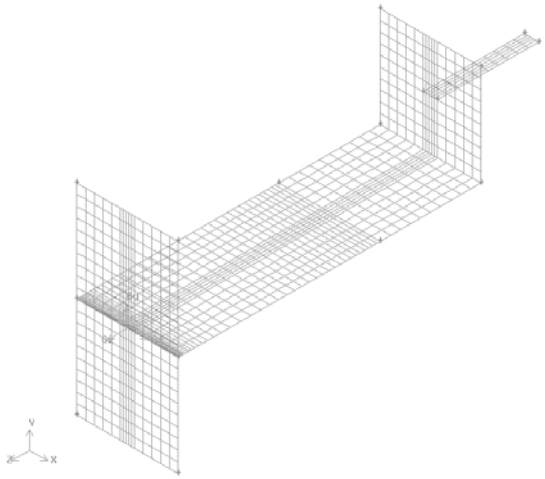

Figure 7: Mesh of the thin steel fixing element

4. Thermo-convective simulation description

4.1 Solver parameters

We used the Fluent software to perform the thermo-convective analysis of the double-skin wall in a stationnary regime. This software is based on a finite volume approach for laminar and turbulent complex flows and is able to deal with structured and unstructured meshes. It allows for the coupled investigations of the thermo-convective flows in the fluid zones and the heat conduction in the solid zones.
In this study, we assumed the air flow is turbulent. This choice relies on the estimate of the so-called Rayleigh number (Ra) which characterizes the natural convection flows. According to its value, the flow is laminar (Ra < 108), transitional (108 < Ra < 1010) or turbulent (1010 < Ra). It is defined as follows:

$$Ra = \frac{c_p g \rho^2 \beta (T_w - T_{out}) L^3}{k\mu}$$

with

- $\mu = 1.87\ 10^{-5}\ Nsm^{-2}$, the air dynamic viscosity at $301.15\ K$
- $c_p = 10^3\ Jkg^{-1}K^{-1}$, the air specific heat at $301.15\ K$
- $k = 2.62\ 10^{-2}\ Wm^{-1}K^{-1}$, the air conduction coefficient at $301.15\ K$
- $\rho = 1.75\ kgm^{-3}$, the air density at $301.15\ K$
- $\beta = 3.33\ 10^{-3}\ K^{-1}$, the air thermal expansion coefficient at $301.15\ K$
- $L = 2\ m$, the panel height
- $T_w - T_{out}$, the temperature difference between the wall and the air zone. It is estimated by assuming an equilibrium between the solar flux applied to the wall ($\alpha\ \phi_{sol} \approx 450\ Wm^{-2}$) and the outgoing flux in both sides of the wall for a constant air temperature ($2\ h_{out}\ (T_w - T_{out}) = 50\ (T_w - T_{out})$). It gives $T_w - T_{out} = 9\ K$.

In these conditions, the Rayleigh number reaches a value of 1010. We made the choice of the k- Є turbulent model. We also selected the following Fluent options in order to model in an accurate way the viscous and the thermal effects in the vicinity of the steel skin :

- Enhanced wall treatment
- Thermal effects
- Viscous heating

Note that the chosen options are not detailed in this report. More explanations can be found in the Fluent User Guide.
In order to investigate the thermal aspects, we explicitly asked Fluent to solve the Energy Equation. We let the default solver option which is the Pressure Based solver. This is recommended when the shell conduction model is used to characterize the thin walls (see below).
The natural convection can be treated in different ways. According to the temperature and density gradients inside of the domain, different modelling approaches exist between the Boussinesq one (for the weakest gradients) and the fully compressible approach (for the highest gradients). We choose the Boussinesq approach without encountering any difficulty. This considers a constant density in the pressure terms of the equations but a free density in the volume terms. This eases the calculation convergence as it avoids the instabilities due to the non-linear terms.

4.2 Materials

The material properties are user-defined as proposed in the table of section 2. The calculation domain is divided in four zones, as shown in figure 3. There are three solid zones, one of insulator material and two of concrete, and a fluid one. As suggested above, the air density property must be turned from constant to Boussinesq. As a consequence, the user must introduce the density and the thermal expansion coefficient at the reference temperature (see the table of section 2).

4.3 Boundary conditions

The following conditions were applied on the external walls of the domain (see figure 8):

- Wall to the planes bounding a solid zone and perpendicular to the y direction. We kept the defaults options as no source is applied.
- Periodic with a null pressure gradient in the y direction to all the faces perpendicular to the x direction, as the investigated domain is supposed to be repeated in the x direction.
- Pressure inlet (outlet) to the lowest (uppermost) face of the air domain, defined by y = −1000 mm (y = +1000 mm). The pressure inlet is the flow entrance and the pressure outlet is supposed to be the flow exit even if a back flow can occur, depending on the local density and temperature properties.

By principle, the natural convection problem has no imposed pressure or velocity conditions.
Therefore, we fixed the total (static) pressure at the inlet (outlet) to the atmospheric pressure, as recommended in this case (see the Fluent User Guide for example). Note that, in order to avoid the round-up error as the pressure variations around the static pressure are small, we defined an operating pressure equal to the atmospheric pressure. This is used as a gauge pressure by Fluent. In the same time, as we forced Fluent to take into account the gravity action, we must not impose the hydrostatic pressure difference between the inlet and the outlet. It will be automatically estimated by Fluent. As a result, we

finally imposed the corrected total (static) pressure at the inlet (outlet) to zero. The velocity is estimated by Fluent at the inlet and the outlet according to the density variations inside of the domain.
The inlet temperature was imposed to the external one (T = 301.15 K) as well as on the outlet face in case of a back flow.
The turbulence parameters were fixed in term of Intensity and length scale (10 % and 2 m).

- Wall with a flux condition on the steel skin. The flux condition is a mixed one as it combines a net flux (Φ_{sol} α (y)) and a convective contribution with the ambient (h_{out} ($T_w - T_{out}$), with T_{out} = 301.15 K) :

$$\phi_{in} = \phi_{sol}\ \alpha(y) - h_{out}\ (T_w - T_{out})$$

Note that even if we did not consider the radiative exchanges inside of the domain, the heat transfer coefficient h_{out} (25 $Wm^{-2}K^{-1}$) is a user-defined coefficient taking into account both the convective and the radiative emission of the steel skin to the ambient.
The heat flux is not constant as the _ coefficient depends on the vertical position and as the unknown T_w changes during the iterative process and with the location on the steel skin. Then, the flux must be defined by a user-defined function (UDF), written in a C-like language. By using the DEFINE PROFILE Macro, it is possible to retrieve each cell temperature on the steel wall and to impose the adequate flux according to the temperature cell and its coordinate. This UDF is called by Fluent at each iteration in order to update the flux profile on the steel plate.
By convention, a positive heat flux is a flux entering the domain. In the first part of the study α is fixed to 0.5. In the second part, two situations are envisaged: α (y) = 0.5 ± 0.4 < y (y = −1, 1m).

Wall with a convection condition on the inner concrete wall to take into account the heat exchange with the indoor. The convective coefficient h_{in} equals to 7.7 $Wm^{-2}K^{-1}$ and the reference temperature inside of the building is 295.15 K.

Fluent estimates the flux by the following relation $\Phi = -h_{in}\ (T_w - T_{in})$ which is an outgoing flux if $T_w > T_{in}$, as imposed by the flux convention.

The internal solid walls (the air/insulator, the insulator/concrete, the concrete/concrete interfaces and the fixing plates) are considered as walls with the default options. As they bound two domains, the option coupled must be activated in order to ensure the flux continuity at the interfaces. Note that if the mesh is correctly generated in Gambit (with connected volumes), this is done automatically.
For the steel fixing planes and the steel skin, which are considered as thin walls, the shell conduction model is selected. This allows solving the conduction problem in the plates without meshing them in the thickness direction. The thickness must be given and the steel material must be selected in order to take into account the plate conduction properties. The steel skin thickness is 2 mm and the thickness of the different fixing parts is given in figure 3.

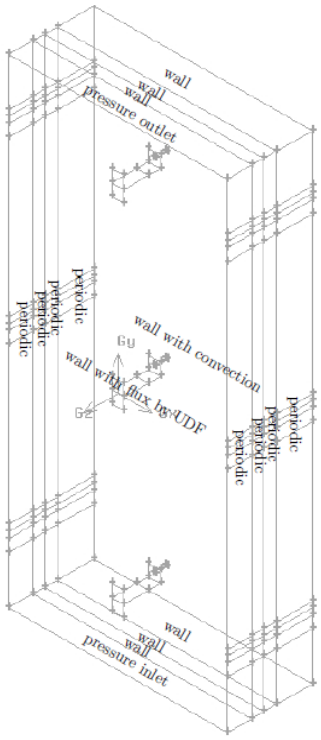

Figure 8: External boundary condition

4.4 Calculation parameters and initialization

To complete the case setup description, we used a second order spatial discretization scheme.
The pressure interpolation scheme was chosen to be Presto ! as recommended by Fluent in the case of a natural convection problem and the pressure-velocity coupling scheme was chosen to be coupled with the default options.

We let all the default under-relaxation parameters, excepted the energy one. It was decreased to 0.8 in order to avoid the appearance of unrealistic residual and temperature oscillations.
These come from the flux dependence on the wall temperature, which strongly varies, especially at the iterative process beginning. By reducing the energy under-relaxation factor, we allow the code to avoid this oscillating behaviour by introducing an artificial inertial effect.

In the operating panel, we imposed the operating pressure to 1 atm as suggested above.
The gravity was activated and imposed to $-9.81\ ms^{-2}$ in the y direction and the reference pressure location was fixed to y = −1 m. The reference temperature for the Boussinesq model was fixed to 301.15 K.
Finally, we initialized the calculation. The initial velocity in the y direction, v_{ini}, was assumed to be $2\ ms^{-1}$. This value is one third of the velocity calculated from the equilibrium between the hydrostatic pressure of the air column and the dynamic pressure, assuming that the inlet velocity is null, which is not exactly true $(\rho g L = \rho v_{ini}^2/2)$
The initial temperature inside of the domain was fixed to 320 K.
The initial turbulent kinetic energy and dissipation rate were fixed to $5000\ m^2s^{-2}$ and $30000\ m^2s^{-3}$ as prescribed by the Fluent User Guide definitions.

4.5 Execution time and convergence monitoring

The process convergence is estimated from the evolution graphs of the residuals, the wall temperatures and the wall fluxes.
One proceeded as follows. We estimated the solution on a rough grid (65000 elements).
This was interpolated on the refined grid and used as the initial solution for the refined case.
The rough solution convergence was reached after 3000 iterations (or 0.5 hour in sequential).
Then, the refined calculation converged after 7500 iterations which took 44 additional hours and 1.5 Gb of memory.

Note that a significant improvement of the convergence rate was reached by continuing the job in double precision. This slightly increased the iteration time but it allowed for turning the energy under-relaxation parameter until 9.975 without the oscillation appearance, so that the convergence rate was faster. This increase of the energy under-relaxation parameter can be done only after a certain solution stabilization.

5. Phase 2: Heat transfer coefficient evolution according to the concrete thickness

The results obtained for the variable-thickness double-skin wall are summarized in the next table, in terms of averaged fluxes (Φ) and temperatures (T) on the inner and the outer faces of the domain. Note we checked that the flux summation on the external faces is almost zero (less than 1% of the flux applied to the steel skin).

Thickness (mm)	Face	$T\ (K)$	$\phi\ (Wm^{-2})$
90	External (steel) skin	317.60	44.14
	Internal (concrete) wall	295.60	-3.41
120	External (steel) skin	317.36	44.14
	Internal (concrete) wall	295.60	-3.38
150	External (steel) skin	317.36	44.14
	Internal (concrete) wall	295.59	-3.35
200	External (steel) skin	317.36	44.13
	Internal (concrete) wall	295.58	-3.30
250	External (steel) skin	317.36	44.13
	Internal (concrete) wall	295.57	-3.24

Table 3: Summary of the variables

With these data, we estimated the heat transfer coefficient U from the averaged flux entering the building (flux on the internal concrete wall, Φ_{conc}) and the averaged temperature difference between the external steel skin and the internal concrete wall ($T_{steel} - T_{conc}$).

Thickness (mm)	$U = \lvert\phi_{conc}\rvert/(T_{steel} - T_{conc})\ (Wm^{-2}K^{-1})$
90	0.157
120	0.155
150	0.154
200	0.151
250	0.149

Table 4: summary of the U value in relation with the thickness

By comparing these coefficients to those of the reference wall (see section 2), we conclude that the double-skin wall configuration brings a significative insulation improvement. Indeed, whatever the thickness concrete, the heat transfer coefficient is 4.5 times lower in the double-skin wall configuration. Note that the comparison with the second column of the same table indicates that the thermo-convective flow decreases of 10 per cent the heat transfer coefficient in comparison with a pure conductive approach taking into account the conduction in the air slab.

These enhancements are due to the flux rejected at the outlet of the air domain. In all the cases the difference between the inlet and the outlet net fluxes is around 75 W, which represents more than 90 per cent of the flux applied to the steel skin.

Figure 9 shows the heat transfer coefficient evolution with the concrete thickness in the double-skin wall configuration. It can be fitted by a similar law than the one we used to estimate the conductive heat transfer coefficient in a 1D approach according to the concrete thickness (see the equation 5). The fitted law is the following

$$U = \frac{1}{a + (e/k')}$$

with e the thickness in meters, k_0 = 0.457 $Wm^{-1}K^{-1}$ the effective thermal conductivity of the double-skin wall , a = $(1/U_0)-(e_0/k_0)$ = 6.1742 m^2KW^{-1}, with U_0 the heat transfer coefficient for a thickness e_0 = 90 10^{-3} m.

The following figures illustrate by different planes the velocity and the temperature in the domain for a 200 mm concrete thickness configuration. Figure 10 shows the temperature map on the steel skin. Figure 11 gives the temperature and the velocity on the centred fixing as well as on the plane y = 0 mm. Figure 12 shows the temperature profiles for different planes in the air slab, the insulation material and the concrete. The considered planes are z = −10 mm (close to the skin), z = −50 mm (middle of the air slab), z = −125 mm (middle of the insulator), z = −150 mm (concrete/insulator interface). In order to catch the characteristics of the temperature profiles, note that the scale is different in the four cases. Figure 13 and 14 show the velocity and the temperature profiles in a stacking view in the planes y = −1000 mm (including the air inlet), y = −500 mm, y = −25 mm (just below a fixing part), y = 25 mm (just above a fixing part), y = 500 mm, y = 1000 mm (including the air outlet). Figures 15 and 16 give the temperature and the velocity profiles on the same planes with a different view.
Figure 17 shows the velocity profiles for different planes in the air slab, the insulation material and the concrete. The considered planes are z = −10 mm (close to the skin) and z = −50 mm (middle of the air slab).
The results reveal that the temperature (and the fluxes) of the inner concrete wall and the steel skin are not significantly affected by the thickness concrete. The temperature on the inner concrete wall is homogeneous - and then not shown on a figure - and close to the indoor temperature (295.15 K), as the outgoing flux is very low. In the steel skin, the temperature is quite homogeneous too due to the high steel thermal conductivity and the constant absorption coefficient. The averaged temperature value is 317.36 K. Note that the temperature is slightly lower close to the air inlet (y = −1000 mm) as we imposed the inlet temperature to 301.15 K.
It is also the case at the fixing junctions. Their high conductivity and their contact with the air zone, cooler than the steel skin, are responsible for this lower temperature. This is shown in figure 11. Moreover, by a thermal bridge effect, the fixing temperature is also different from the surrounding one, either higher in the air zone, or lower in the insulation material. In the insulation material, the fixing temperature reaches the concrete temperature after few millimetres, so that the fixings do not impact the concrete temperature, whatever the concrete thickness.
The thermal effect of the steel fixing, especially how they impact their surrounding, are also illustrated in figure 12, for several z planes.

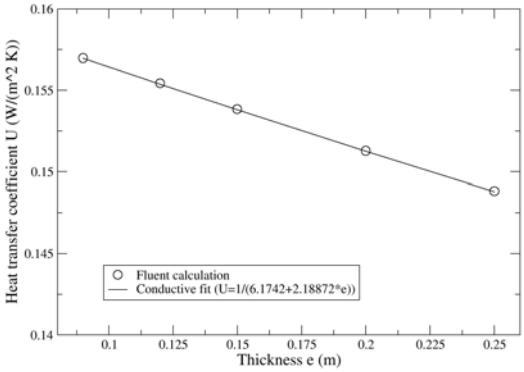

Figure 9: Evolution of the heat transfer coefficient of the double-skin wall with the concrete

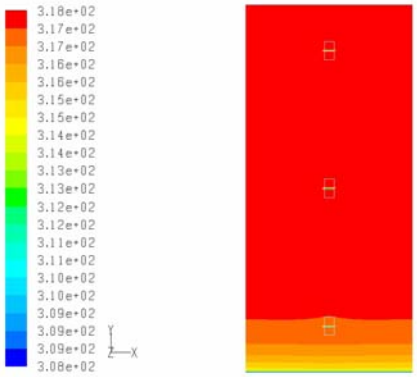

Figure 10: steel skin temperature [K]

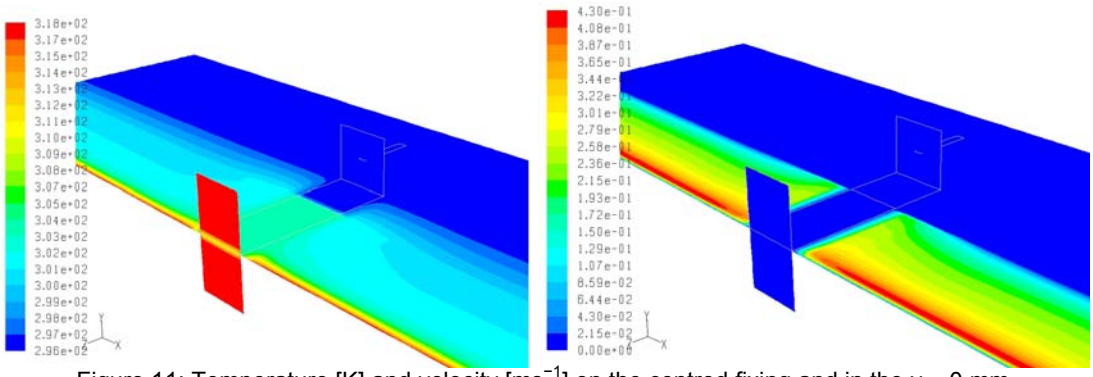

Figure 11: Temperature [K] and velocity [ms^{-1}] on the centred fixing and in the y = 0 mm ***plane.***

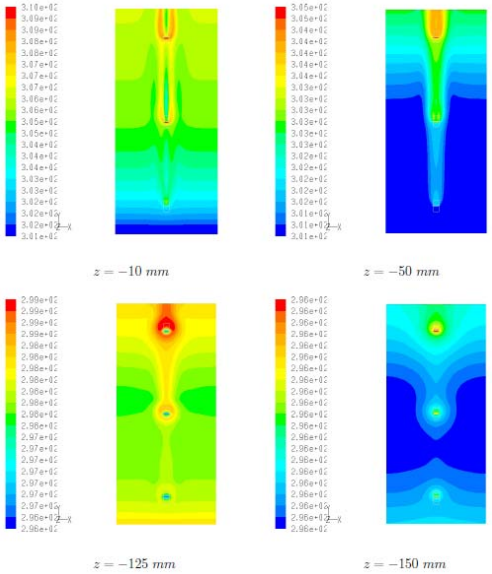

Figure 12: Temperature [K] profiles in several z planes. Note that the temperature scale is adapted to each case in order to highlight the characteristics of each case.

As shown in figures 11, 13, 14, 15 and 16, the temperature and the velocity gradients in the z direction are large in the vicinity of the skin wall, as expected. At the inlet face, the velocity and the temperature are constant due to the boundary conditions we imposed. Indeed, imposing the total pressure at the inlet is responsible for a constant, but non-zero, velocity profile at the inlet.

The velocity increases with the vertical coordinate, especially at the vicinity of the skin wall, as shown in figure 17. It reaches its maximum value (0.47 ms^{-1}) close the uppermost steel fixing. Note that the estimated mass flow at the inlet and the outlet faces is 2.31 10^{-2} kgs^{-1}.

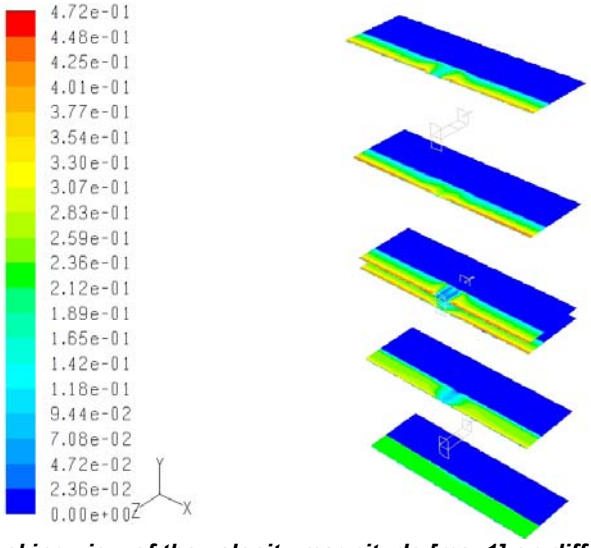

Figure 13: Stacking view of the velocity magnitude [ms−1] on different y planes.

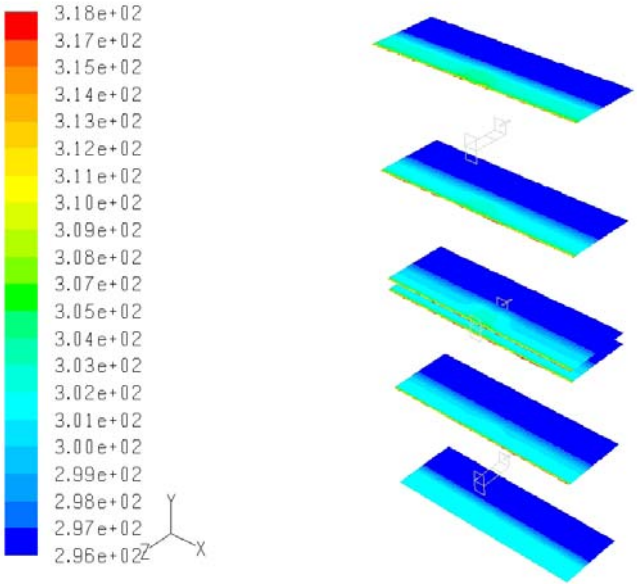

Figure 14: Stacking view of the temperature magnitude [K] on different y planes.

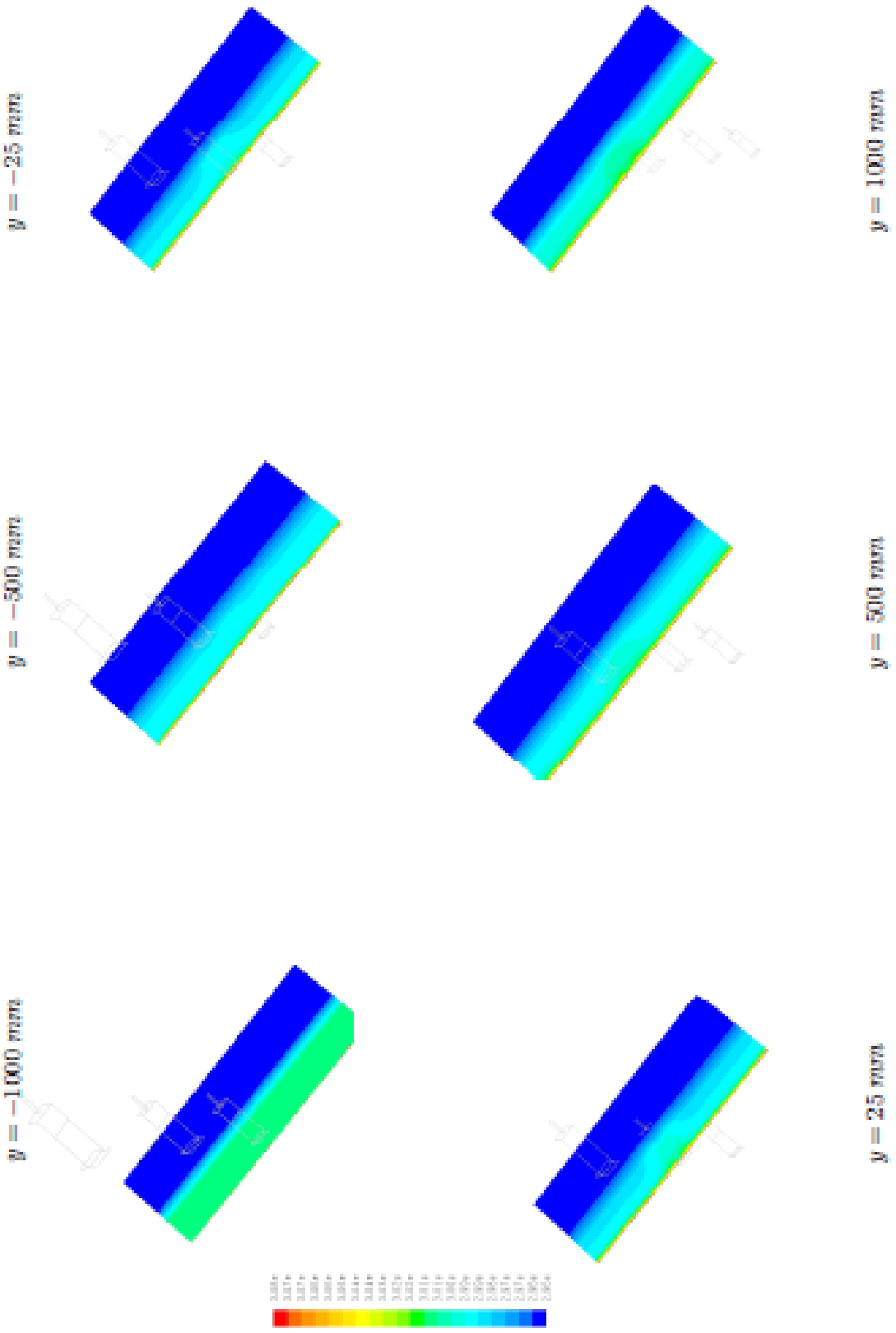

Fig. 15 – Temperature [K] profiles in several y planes.

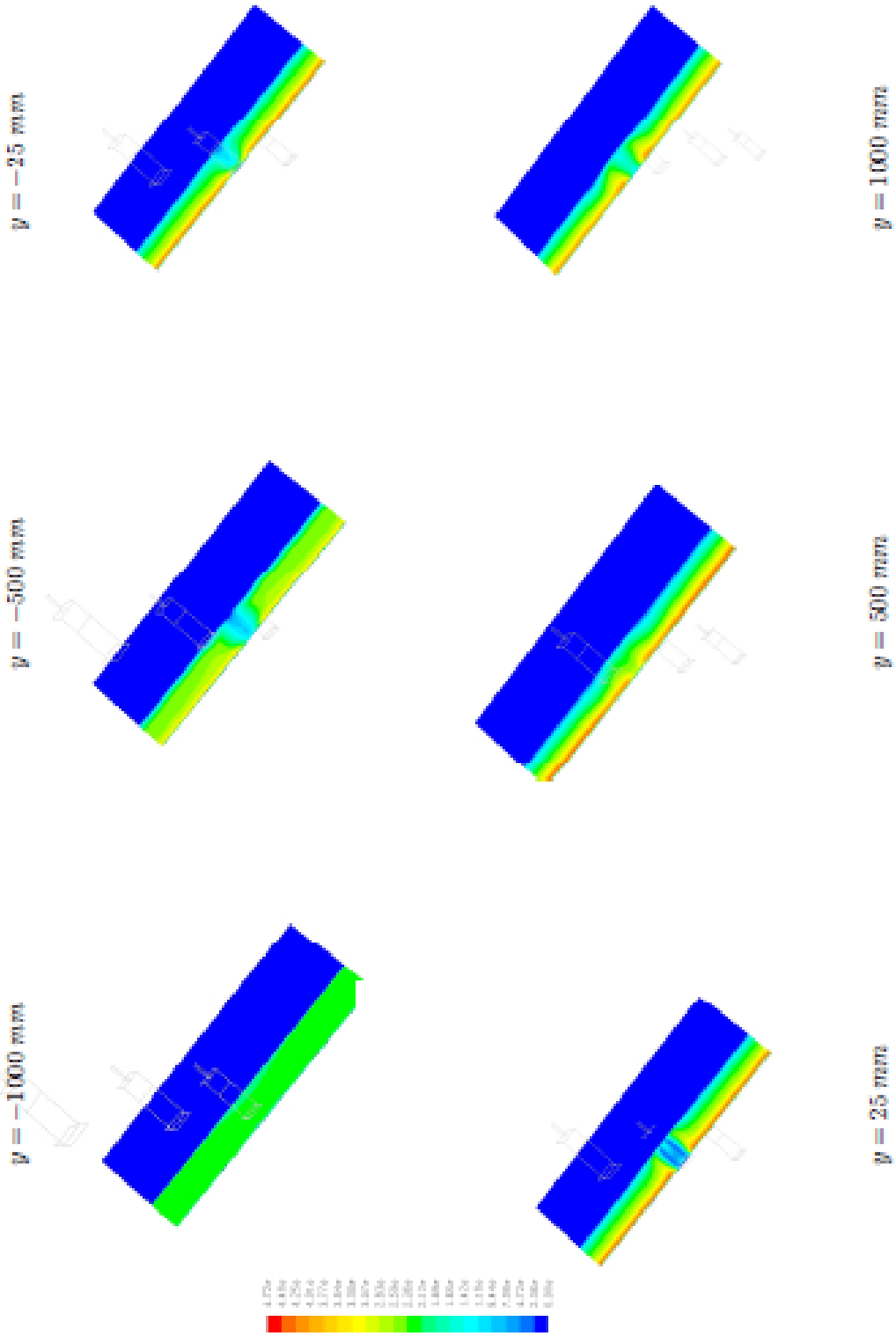

Fig. 16 – Velocity [$m.s^{-1}$] profiles in several y planes.

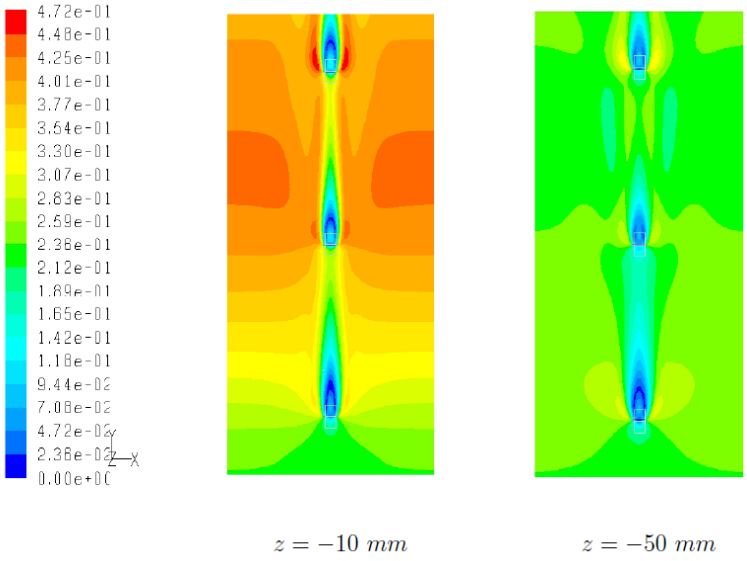

Figure 15: Velocity profiles in two z planes

Figure 17 suggests that the flow is almost parallel to the vertical direction. This is confirmed by the velocity pathlines proposed in figure 18 and 19. Note that the fixings locally disturb the flow. As the turbulence effects are small inside of the domain, the symmetry of the flow is not affected, so that we could have chosen a symmetric approach instead of a periodic one to treat the x direction.

Figure 20 illustrates the same velocity pathlines, issued from the outlet faces. We can see that a back flow occurs close to the insulation wall due to the local temperature and density properties.

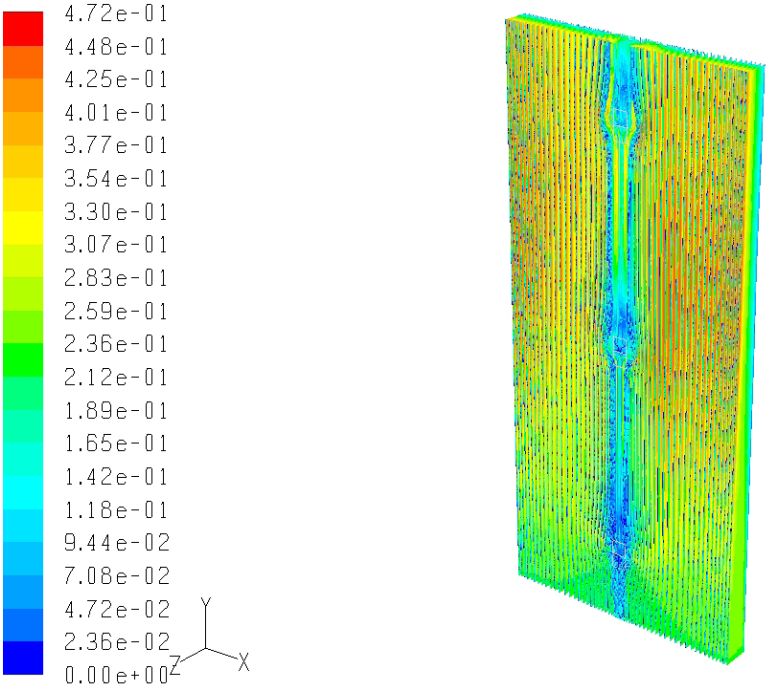

Figure 16: Velocity pathlines issued from the inlet face [ms−1]

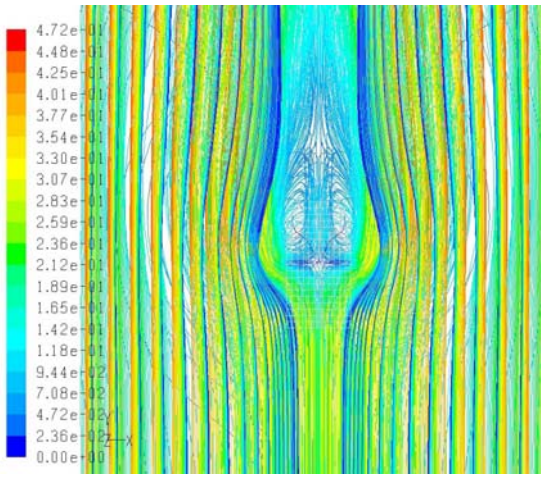

Figure 17: Velocity pathlines issued from the inlet face [ms−1] : zoom on the centred fixing

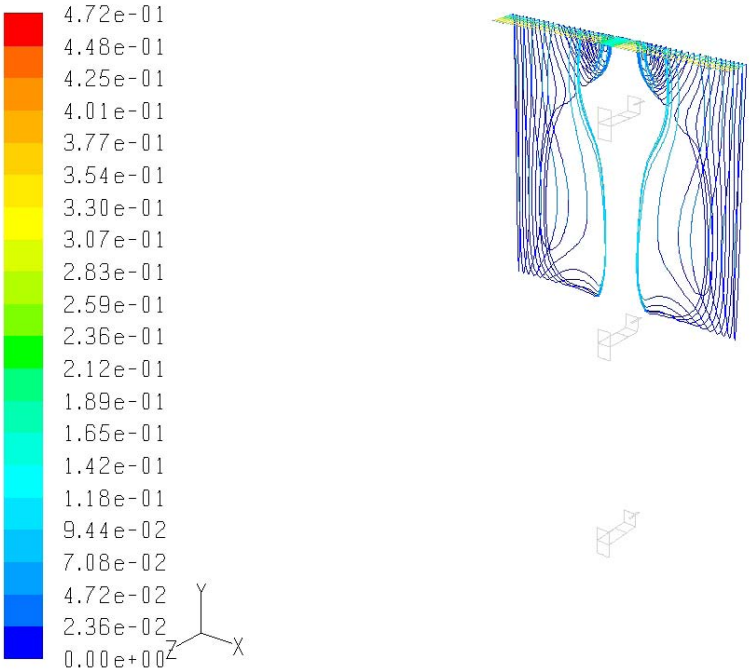

Figure 18: Velocity pathlines issued from the outlet face [ms−1]

6. Double skin façade and HVAC systems- application

As Stec et al., (2003) describe, an HVAC system can be used in the three following ways in a Double Skin Façade office building:

- Full HVAC system (the Double Façade is not a part of the HVAC) which can result in high energy use. On the other hand, the user can select whenever he prefers a controlled mechanically conditions inside or natural ventilation with the use of the Double Skin Façade).
- Limited HVAC system (the Double Façade contributes partly to the HVAC system or is playing the major role in creating the right indoor climate). In this way the Double Façade can play the role of
    - o the pre-heater for the ventilation air
    - o ventilation duct
    - o pre-cooler (mostly for night cooling)
- No HVAC. The Double Facade fulfills all the requirements of an HVAC system. This is the ideal case that can lead to low energy use.

[1] During the heating periods the outdoor air can be inserted from the lower part of the façade and be preheated in the cavity (figure 19). The exterior openings control the air flow and thus the temperatures.

Then, through the central ventilation system the air can enter the building at a proper temperature. During the summer, the air can be extracted through the openings from the upper part of the façade. This strategy is applied usually to multi storey high Double Skin Facades. This type provides better air temperatures during the winter but during the summer the possibility of overheating is increased.

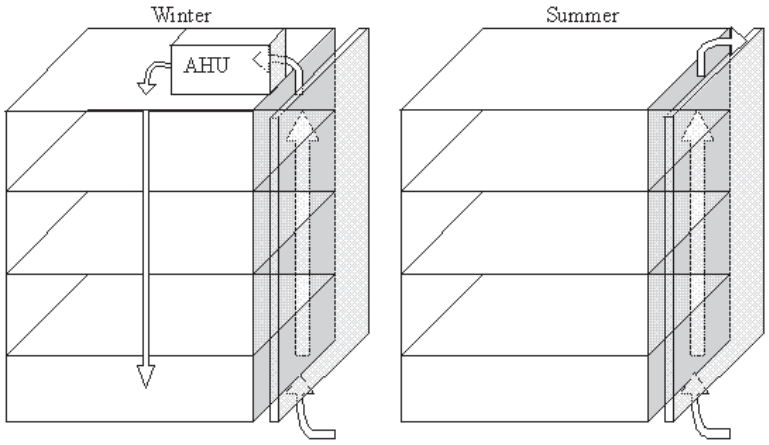

Figure 19: Double skin façade and HVAC [1]

During the whole year, the double skin façade cavity can be used only as an exhaust duct without possibility of heat recovery for the HVAC system (figure 20). It can be applied both during winter and summer to the same extent. The main aim of this configuration is to improve the insulation properties in the winter and to reduce the solar radiation heat gains during the summer. There are no limitations in individual control of the windows' openings.

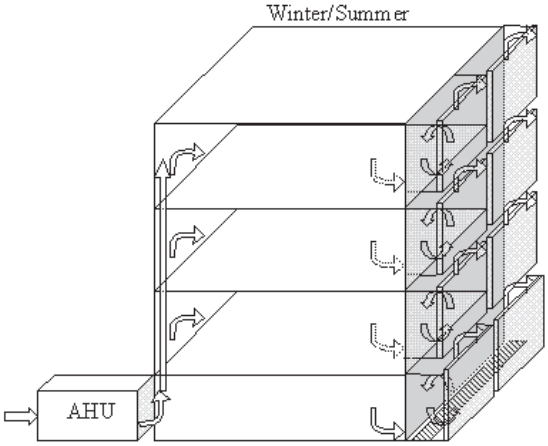

Figure 20: double skin façade as an exhausting duct [1]

The possibility to use the Double Skin Façade as an individual supply of the preheated air also exists (figure 21). This strategy can be applied both in multi-storey and box window type. An exhaust ventilation system improves the flow from the cavity to the room and to exhaust duct.
Extra conditioning of air is needed in every room by means of VRV system or radiators. This solution is not applicable for the summer conditions since the air temperature inside the cavity is higher than the thermal comfort levels. Also in this case there are no limitations in individual control of the windows' openings.

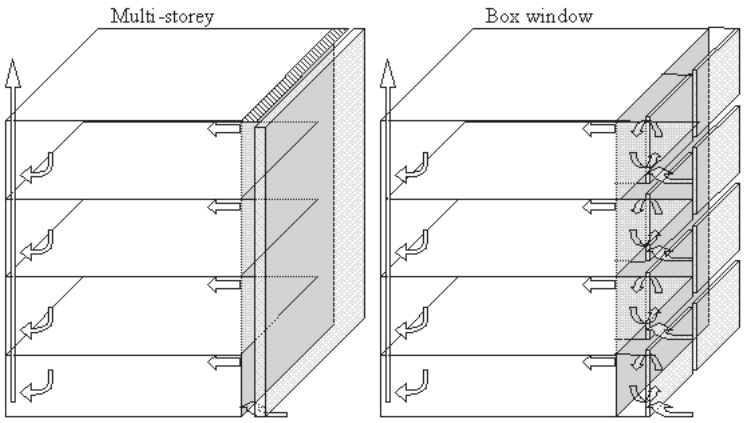

Figure 21: Double Skin Façade as an individual supply of the preheated air. [1]

Finally, the Double Skin Façade cavity can be used as a central exhaust duct for the ventilation system (figure 22). The air enters through the lower part of the cavity and from each floor. Supply ventilation system stimulates the flow through the room to the cavity. The recovery of air is possible by means of heat pump or heat regenerator on the top of the cavity. The windows cannot be operable due to the not fresh air in the cavity.

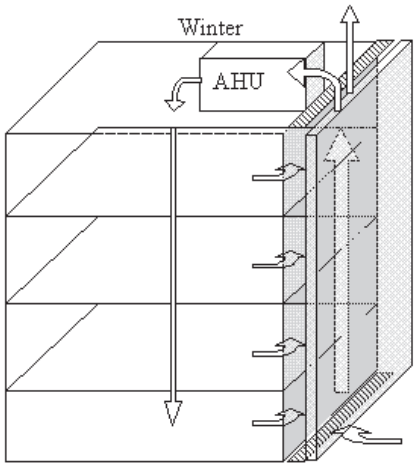

Figure 22: Double Skin Façade as a central exhaust duct for the ventilation system [1].

6.1 Advantages & Disadvantages- Literature based [1]

Disadvantages mentioned by author	Oesterle et al. (2001)	Compagno (2002)	Claessens et al.	Lee et al. (2002)	B.B.R.I. (2002)	Arons (2000)	Faist (1998)	Kragh, (2000)	Jager (2003)
Higher construction costs	√				√	√			√
Fire protection	√				√				√
Reduction of rentable office space	√								√
Additional maintenance and operational costs	√		√		√				√
Overheating problem	√	√			√		√		√
Increased air flow speed					√				
Increased weight of the structure			√						√
Daylight	√								
Acoustic insulation	√				√				√

Advantages mentioned by author	Oesterle et al., (2001)	Compagno, (2002)	Claessens et al.	Lee et al., (2002)	B.B.R.I., (2002)	Arons, (2000)	Faist, (1998)	Kragh, (2000)	Jager, (2003)
Lower construction cost (comparing to electrochromic, thermochromic photochromic panes)	√								
Acoustic insulation	√			√		√	√	√	√
Thermal insulation during the winter	√	√		√	√		√	√	
Thermal insulation during the summer	√	√		√			√	√	
Night time ventilation	√	√	√	√		√			
Energy savings and reduced environmental impacts						√			
Better protection of the shading or lighting devices	√	√		√					√
Reduction of the wind pressure effects	√	√	√						√
Transparency – Architectural design				√	√	√		√	
Natural ventilation	√	√		√		√	√		√
Thermal comfort – temperatures of the internal wall	√	√		√	√	√	√	√	
Fire escape	√								
Low U-Value and g-value		√				√		√	

7. Conclusions

In this work, we investigated the thermo-convective flow in a double-skin wall based on the stacking of a thin steel wall, an air slab and a solid wall made of an insulation material and concrete. We examined the natural convection phenomenon in the air layer and the heat transfer in the fluid and the solid zones, included in the thin steel wall and the fixings that ensure the assembly stiffness.

We found that the double-skin configuration decreases the heat transfer coefficient of a factor 4.5 in comparison with a reference wall made of an insulator and concrete, whatever the concrete thickness. This improvement is due to the natural convection process that takes place in the air slab and evacuates a large amount of the heat load applied to the steel skin.

The evolution of the heat transfer with the concrete thickness remains linear, as in a pure conductive problem. Then we were able to define an effective thermal conductivity which is much lower than the concrete one. We found that the fixings play a secondary thermal role and they do not impact the global heat transfer even for a small concrete thickness.

8. Bibliography

I. Harris Poirazis (2004), Double Skin Façades for Office Buildings, Report EBD-R--04/3
II. BBRI (2002),Source book of the Belgian Building Research Institute
III. Harrison and Boake (2003),Tectonics of the Environmental Skin
IV. Arons, (2001)
V. Claessens and DeHerde
VI. Kragh, (2000)
VII. Cenario :OP/2007/46/ARCELOR/1/MUR2PEAU/REPORT-V1
VIII. Stec et al., (2003)

Saelens D., Roels S. & Hens H. (2003), on the influence of the inlet temperature in multiple skin façade modelling